SIMULATION OF IDEAL EXTERNAL AND INTERNAL FLOWS WITH ARBITRARY BOUNDARIES USING SCHWARZ-CHRISTOFFEL TRANSFORMATION

S. H. Mansouri and M.A. Mehrabian

Department of Mechanical Engineering, Shahid Bahonar University of Kerman, P.O. Box 76169 - 133, Kerman, Iran, ma_mehrabian@mail.uk.ac.ir

S.M. Hosseini Sarvari

Department of Mechanical Engineering, Sistan and Baluchestan University, P.O. Box 98135-161, Zahedan, Iran

(Received: August 4, 2003 – Accepted in Revised Form: July 10, 2004)

Abstract The flow field, velocity and pressure coefficient distribution of some 2-D ideal flows are presented. Conformal mapping is used to simulate two-dimensional ideal flow for a variety of complex internal and external configurations, based on the numerical integration of Schwarz-Christoffel transformation. The advantages of this method are simplicity and high accuracy. The method presented in this paper has been applied to flow problems for which established experimental results are available in the literature. The close agreement between the predictions of simulation program and experimental results shows that the present method is applicable to any 2-D ideal flow regardless of the system of coordinates.

Keywords Ideal Flow, Conformal Mapping, Schwarz-Christoffel Transformation.

چکیده در این مقاله میدان جریان، مولفه های سرعت و ضریب فشار بعضی جریان های ایده آل با استفاده از نگاشت همدیس بدست می آیند. این روش همچنین برای شبیه سازی انواع جریان های ایده آل داخلی و خارجی پیچیده در حالت دوبعدی مورد استفاده قرار می گیرد. روش نگاشت همدیس مبتنی بر انتگرال گیری عددی از تبدیل شوارتز–کریستوفل می باشد. مزایای این روش عبارتند از سادگی و دقت زیاد. روش ارائه شده در این مقاله در مورد مسائلی که نتایج تجربی منتشر شده در مقالات معتبر علمی دارند بکار گرفته شده است. مطابقت نزدیک بین پیش بینی های برنامه شبیه سازی و نتایج تجربی نشان می دهد که روش حاضر در مورد تمام جریان های ایده آل دوبعدی بدون درنظر گرفتن هندسه جریان قابل استفاده است.

1. INTRODUCTION

The solution of two-dimensional ideal flow over arbitrary boundaries can be obtained solving Laplace's equation by numerical methods (FDM or FEM). These methods are carried out in four stages: (1) specification of the domain, (2) generation of the boundary-conforming grid, (3) discretization of the differential equation to form a set of algebraic equations and (4) solution of the set of algebraic equations. Discretization processes introduce truncation error. The round-off error is introduced due to numerical calculation, which may lead to substantial error in the solution [1,2].

The linearized potential equation is solved efficiently by the panel method and is accurate for subsonic flow. However, using panel method, a solution for the body pressure distribution can be obtained without solving the flow field throughout the domain. In this case, the problem is reduced to the solution of a system of algebraic equations for source, doublet, or vortex strengths on the boundaries. Panel methods require the solution of a large system of algebraic equations. However, the number and position of surface panels is essential in obtaining a good solution for the body surface pressure [3].

Traditionally, conformal mapping has been used to obtain potential flow solution about relatively complicated shapes by knowing the flow behavior about simple shapes, such as a circle with unit radius [4]. Conformal mapping is used as a grid generation technique with no restriction on the type of flow [5-7]. In practice, the generated grid lines may be chosen to coincide with the streamlines of an equivalent potential flow problem. This feature is often in favor of stability of the computational method used to solve more general problems. Mansouri et al. [8] used simple mappings for generating orthogonal grid over a variety of shapes in external flows. They also applied Schwarz-Christoffel transformation as a powerful tool for generating two-dimensional boundary-conforming grid [9].

In this paper, conformal mapping techniques based on Schwarz-Christoffel transformation are presented to solve two-dimensional ideal flow over arbitrary boundary shapes. In this method, the components of the velocity *(u,v)* and the pressure coefficient , C_p , are obtained as analytical functions of ideal flow parameters (ϕ,ψ) over the whole domain. Hence, there is no truncation error as compared with traditional numerical methods. Since the pressure distribution of ideal flow and boundary layer flow coincide, the pressure distribution obtained from this method for the ideal flow, can be incorporated into the boundary layer momentum equation. The data obtained for velocity and pressure distribution can be used as the elementary solution for iterating methods to solve two-dimensional viscous flow. This technique is accurately applicable for simply-connected or symmetrical multiply-connected regions in external and internal flows.

2. PROBLEM FORMULATION

2.1 External Flow Schwarz-Christoffel transformation for external flow geometries can be described as mapping of a polygon in *z(x,y)*–plane onto the upper half of $w(\phi,\psi)$–plane (see Figure 1). Boundary of the polygon will correspond to real axis of *w*-plane. The structure of the Schwarz-Christoffel transformation for external flows is as follows:

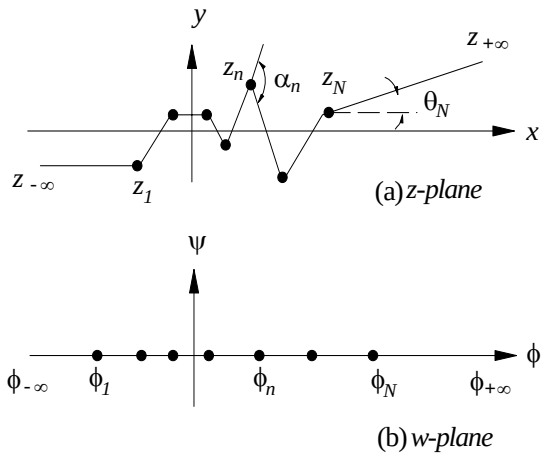

Figure 1. Mapping of a polygon in *z(x,y)*–plane onto the upper half of $w(\phi,\psi)$–plane.

$$\frac{dz}{dw} = A\prod_{n=1}^{N}(w-\phi_n)^{-\alpha_n/\pi} \qquad (1)$$

where N is the number of polygon apices and α_n is the angle of counterclockwise rotation at each apex. The points ϕ_n are unknown positions on the real axis in *w*-plane, where each of them corresponds to an apex of the polygon in *z*-plane. A is a complex constant which depends on the geometry of physical domain. Correct selection of points ϕ_n involves an iterative numerical procedure. According to Riemann theorem [4], the positions of three points of ϕ_n are arbitrary. It is possible to use Equation 1 for a polygon with $N+1$ sides in *z*-plane where its $N+1^{th}$ apex is at $\pm\infty$, and the values of $\phi_{\pm\infty}$ corresponding to $z_{\pm\infty}$, are removed from Equation 1.

The mapping function of $z(w)$ may be obtained, integrating Equation 1 as follows :

$$z(w) = A\int_{w_0}^{w}\prod_{n=1}^{N}(w-\phi_n)^{-\alpha_n/\pi}\,dw + B \qquad (2)$$

where w_0 is a point on the upper half of *w*-plane , and B is a complex constant. Correct selection of points ϕ_n involves an iterative procedure [9]. This procedure is based on two consecutive mappings,

as follows:

$$s(w) = \int_{w_0}^{w} \prod_{n=1}^{N} (w - \phi_n)^{-\alpha_n/\pi} dw \quad (3)$$

$$z(s) = As + B \quad (4)$$

One can assume the following initial values for ϕ_n:

$$\phi_n^1 = \begin{cases} 0 & if \quad n = 1 \\ \phi_{n-1}^1 + \left| z_n^c - z_{n-1}^c \right| & if \quad n = 2,3,..., N \end{cases} \quad (5)$$

where superscript *c* shows the convergence value. ϕ_n^1 can be normalized by the following transformation :

$$\phi_n^1 = 2\frac{\phi_n^1}{\phi_N^1} - 1 \quad (6)$$

Due to singular nature of Equation 3 at points $w=\phi_n$, the integration path can be located at $w+i\varepsilon$ in the *w*-plane, where ε has a very small value (e.g. 10^{-10}). In order to speed up the integration process of Equation 3, the following procedure is used for determining s_m^{υ}:

$$s_m^{\upsilon} = \begin{cases} 0 & if \quad m = 1 \\ s_{m-1}^{\upsilon} + \int_{\phi_{m-1}^{\upsilon}}^{\phi_m^{\upsilon}} \prod_{n=1}^{N} (w + i\varepsilon - \phi_n^{\upsilon})^{-\alpha_n/\pi} dw \end{cases} \quad (7)$$

where υ is the iteration index. Henceforth, to correct the position of polygon apieces on *z*-plane, in each iteration, the following procedure is used:

$$z_m^{\upsilon} = A^{\upsilon} s_m^{\upsilon} + B \qquad m = 1,2,..., N \quad (8)$$

where,

$$\begin{cases} A^{\upsilon} = \dfrac{Max\left| z_1^c - z_n^c \right|}{\left| s_1^{\upsilon} - s_n^{\upsilon} \right|} e^{i\theta_N} \quad n = 2,3,..., N \\ B = z_1^c \end{cases} \quad (9)$$

where the superscript *c* denotes the exact value. θ_N is the angle between the last side of polygon with horizon. A^{υ} is a scale ratio between *z*-plane to *s*-plane and *B* maps the point u_1 onto the point z_1^{υ}. The structure of Schwarz-Christoffel transformation is such that it will preserve the polygon apex angles at each iteration. Hence, the location of polygon apieces should be corrected by an iteration procedure. The error criterion for all points is the difference between z_m^{υ} and z_m^c that is:

$$err_m^{\upsilon} = \left| z_m^{\upsilon} - z_m^c \right| < \varepsilon \quad m = 1,2,..., N \quad (10)$$

where ε is a small value. The iteration process will be continued until the above criterion is satisfied. To correct the difference between the points $\phi_n^{\upsilon+1}$ for next iteration, the following procedure will be used:

$$\phi_n^{\upsilon+1} = \begin{cases} 0 & if \qquad n = 1 \\ \phi_{n-1}^{\upsilon+1} + \dfrac{\left| z_n^c - z_{n-1}^c \right|}{\left| z_n^{\upsilon} - z_{n-1}^{\upsilon} \right|} (\phi_n^{\upsilon} - \phi_{n-1}^{\upsilon}) \end{cases} \quad (11)$$

and $\phi_n^{\upsilon+1}$ can be normalized by the following transformation:

$$\phi_n^{\upsilon+1} = 2\frac{\phi_n^{\upsilon+1}}{\phi_N^{\upsilon+1}} - 1 \quad (12)$$

Then, referring to Equation 7, the whole process should be repeated to converge.

2.2 Internal Flow Internal flow geometries can be described as a polygon with *N+1* sides on the physical plane, where *M* sides locate on the lower part of the boundary and *P* sides locate on the upper part of the boundary ($N + 1 = M + P$), such that the two apieces are at $\pm\infty$. This polygon will be mapped onto the real axis of *s*-plane such that the vertex z_{M+1} being mapped onto the points σ_{M+1} and the apex at z_{N+1} being mapped to the points $\sigma_{N+1} = \pm\infty$ at the real axis of *s*-plane.

$$\frac{dz}{ds(w)} = A\prod_{n=1}^{N} \left[s(w) - \sigma_n \right]^{-\alpha_n/\pi} \quad (13)$$

where,

$$s(w) = e^{w} \tag{14}$$

N is the number of polygon apices and α_n is the angle of counterclockwise rotation at each apex (see Figure 2). The points σ_n are unknown positions on the real axis in s-plane and A is a complex constant.

The mapping function $z(s)$ may be obtained by integrating Equation 13 as follows:

$$z(s) = A\int_{s_0}^{s} \prod_{n=1}^{N} (s-\sigma_n)^{-\alpha_n/\pi}\, ds + B \tag{15}$$

where s_0 is an arbitrary point in the upper part of s-plane , and B is a complex constant. As for external flows, correct selection of points σ_n involves an iterative numerical procedure.

Like external flows, Equation 15 must be integrated by an initial assumption for the distribution of σ_n on the real axis of s-plane.

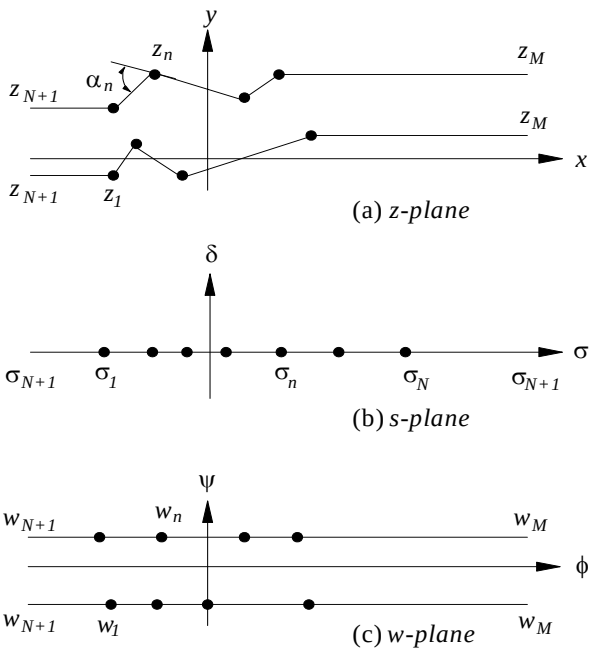

Figure 2. Mapping of a polygon in $z(x,y)$–plane and $w(\phi,\psi)$–plane onto the upper half of $s(\phi,\psi)$–plane.

Knowing the location of convergence points (z_n^c) on the physical plane, the following initial values for σ_n^1 can be used:

$$\sigma_n^1 = \begin{cases} -n & if \quad n = 1,2,..., M \\ 0 & if \quad n = M+1 \\ n & if \quad n = M+2,..., N \end{cases} \tag{16}$$

and corrected by;

$$\sigma_n^1 = \begin{cases} \sigma_{n-1}^1 - \left| z_n^c - z_{n-1}^c \right| & if \quad n = 1,2,..., N_1 \\ \sigma_{n-1}^1 + \left| z_n^c - z_{n-1}^c \right| & if \quad n = N_1+2,..., N \end{cases} \tag{17}$$

However, there is a problem at point $z_{N_1+1} \to \infty$. This problem may be solved by taking an arbitrary value for z_{N_1+1}. Since the value of z_{N_1+1} will only be used to guess a value for σ_n, it may be assumed

$$z_{M+1}^c = 1 + \frac{1}{2}\left(z_M^c + z_{M+2}^c\right) \tag{18}$$

To obtain the points z_m^{υ} corresponding to σ_m^{υ}, Equation 15 should be integrated numerically. In order to speed up the integration process, the following procedure will be used for determining z_m^{υ} :

$$z_m^{\upsilon} = \begin{cases} z_m^c & if \quad m = 1 \\ z_{m-1}^{\upsilon} + A\int_{\sigma_{m-1}^{\upsilon}}^{\sigma_m^{\upsilon}} \prod_{n=1}^{N} (s+i\varepsilon-\sigma_n^{\upsilon})^{-\alpha_n/\pi}\, ds + B \end{cases} \tag{19}$$

and

$$\begin{cases} A = -\dfrac{h}{\pi} \\ B = z_1^c \end{cases} \tag{20}$$

where h is the distance between lower and upper walls of a conduit. Since, the value of z_{M+1}^{υ} will only be used to correct the value of $\sigma_n^{\upsilon+1}$, the

following relation can be used for each iteration:

$$z_{M+1}^{\upsilon} = z_{M+1}^{c} \tag{21}$$

The error criterion is:

$$err_m^{\upsilon} = \left| z_m^{\upsilon} - z_m^{c} \right| < \varepsilon \qquad m=1,2,...,N \tag{22}$$

To correct the distance between the points $\sigma_n^{\upsilon+1}$ for next iterations, the following relations are used:

$$\sigma_n^{\upsilon+1} = \begin{cases} \sigma_1^{\upsilon} & if \quad n=1 \\ \sigma_{n-1}^{\upsilon+1} + \dfrac{\left| z_n^{c} - z_{n-1}^{c} \right|}{\left| z_n^{\upsilon} - z_{n-1}^{\upsilon} \right|} (\sigma_n^{\upsilon} - \sigma_{n-1}^{\upsilon}) \end{cases} \tag{23}$$

corrected by

$$\sigma_n^{\upsilon+1} = \sigma_n^{\upsilon+1} - \sigma_{M+1}^{\upsilon+1} \tag{24}$$

Henceforth, referring to Equation 19, the whole processes should be repeated to converge.

3. CALCULATION OF IDEAL FLOW SPECIFICATIONS

Let complex variable $z = x+iy$ indicates the coordinates of the solution domain (physical plane) and $w(z) = \phi(x,y) + i\psi(x,y)$ is the complex potential function of ideal flow. ϕ and ψ are potential and stream functions respectively, so that

$$u = \phi_x = \psi_y \,,\; v = \phi_y = -\psi_x \tag{25}$$

where u and v are the horizontal and vertical components of velocity in x and y directions, respectively. Then,

$$\frac{dz}{dw} = \frac{1}{V^2}(u + iv) \tag{26}$$

where V is the magnitude of flow velocity. Since $dw/dz = u - iv$, from Equation 26 we have:

$$V = \frac{1}{\left| dz/dw \right|} \tag{27}$$

hence,

$$u + iv = \frac{dz/dw}{\left| dz/dw \right|^2} \tag{28}$$

Using Bernoulie equation, the pressure coefficient C_p becomes,

$$C_p = \frac{P}{\frac{1}{2}\rho V_\infty^{\,2}} = 1 - (\frac{V}{V_\infty})^2 \tag{29}$$

where V_∞ is the upstream velocity, its magnitude is equal to unity. Substituting Equation 27 into Equation 29 we have,

$$C_p = 1 - \frac{1}{\left| dz/dw \right|^2} \tag{30}$$

3.1 External Flow The components of velocity will be determined by Substituting Equation 1 into Equation 28 as follows:

$$u_e(\phi,\psi) + iv_e(\phi,\psi) = \frac{\prod_{n=1}^{N} (w-\phi_n)^{-\alpha_n/\pi}}{\left| \prod_{n=1}^{N} (w-\phi_n)^{-\alpha_n/\pi} \right|^2} \tag{31}$$

The pressure coefficient can be determined by substituting Equation 1 into Equation 30 as follows:

$$C_{p_e}(\phi,\psi) = 1 - \frac{1}{\left| \prod_{n=1}^{N} (w-\phi_n)^{-\alpha_n/\pi} \right|^2} \tag{32}$$

where subscript e indicates the external flow.

3.2 Internal Flow From Equations 13 and 14, the final transformation from w-plane to z-plane is:

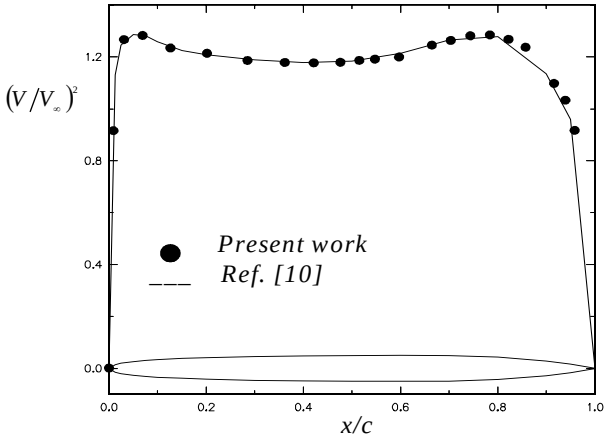

Figure 3. Typical chordwise squared velocity ratio for airfoil NACA0010-66.

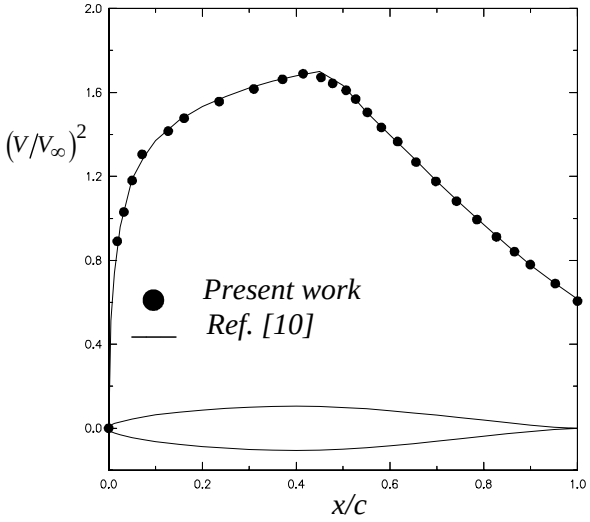

Figure 4. Typical chordwise squared velocity ratio for airfoil $NACA65_4$-021.

$$\frac{dz}{dw}=\frac{dz}{ds}\times\frac{ds}{dw}=\left(A\prod_{n=1}^{N}(e^{w}-\sigma_n)^{-\alpha_n/\pi}\right)e^{w} \tag{33}$$

The components of velocity will be determined by substituting Equation 33 into Equation 28 as follows:

$$u_i(\phi,\psi)+iv_i(\phi,\psi)=\frac{\prod_{n=1}^{N}(e^{w}-\sigma_n)^{-\alpha_n/\pi}e^{w}}{\left|\prod_{n=1}^{N}(e^{w}-\sigma_n)^{-\alpha_n/\pi}e^{w}\right|^2} \tag{34}$$

The pressure coefficient can be determined by substituting Equation 33 into Equation 30 as follows:

$$C_{p_i}(\phi,\psi)=1-\frac{1}{\left|\prod_{n=1}^{N}(e^{w}-\sigma_n)^{-\alpha_n/\pi}e^{w}\right|^2} \tag{35}$$

where subscript *i* indicates the internal flow.

4. RESULTS AND DISCUSSION

4.1 External Flow To check the performance and accuracy of the present method to simulate the ideal external flows, two test cases are considered. Figure 3 shows the distribution of $(V/V_\infty)^2$ for NACA0010-66 airfoil. It can be seen that the results obtained from the above procedure are in good agreement with the experimental results from [10]. In Figure 4, a comparison between the present methods with experimental results from [10] for another standard airfoil is shown. It can be seen that the two sets of results are in good agreement. Table 1 shows the cpu time to converge, number of iterations and the maximum error for two cases.

In Figures 5 and 6, velocity vectors, streamlines and pressure coefficient contours for ideal flow over a car profile corresponding to two different domains are shown. As seen, the solution of ideal flow by this method is independent of the coordinates of solution domain.

In Figure 7 the pressure coefficient contours for ideal flow over arbitrary smooth curve is shown. The distribution of ideal flow characteristics over the surface is shown in Figure 8.

4.2 Internal Flow Figure 9 shows the pressure

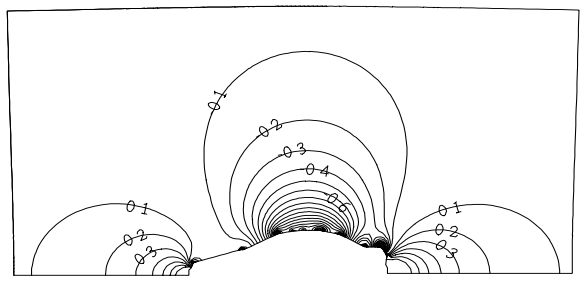

(a)

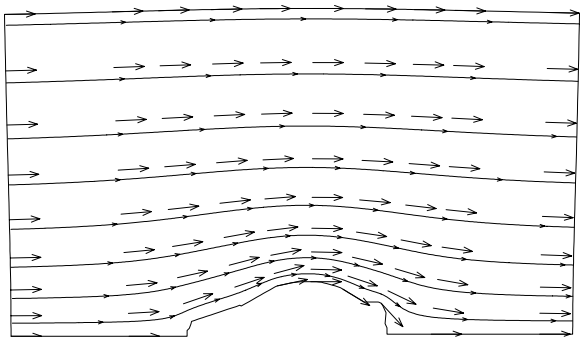

(b)

Figure 5. (a) C_p contours and (b) velocity vectors and streamlines for ideal flow over a car profile.

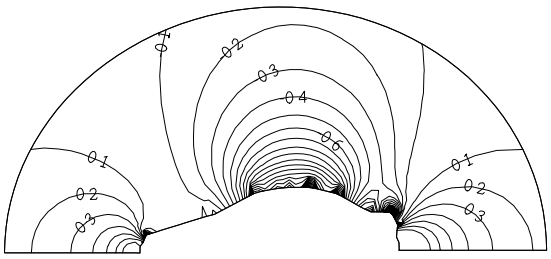

(a)

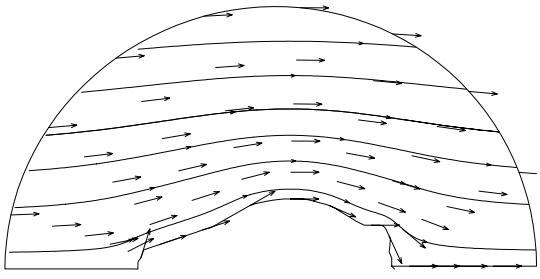

(b)

Figure 6. (a) C_p contours and (b) Velocity vectors and streamlines for ideal flow over a car profile corresponding to an alternative solution domain.

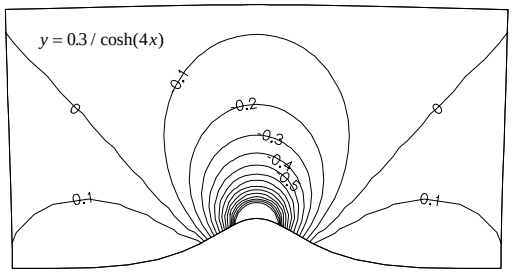

Figure 7. C_p contours for a smooth curve in external flow.

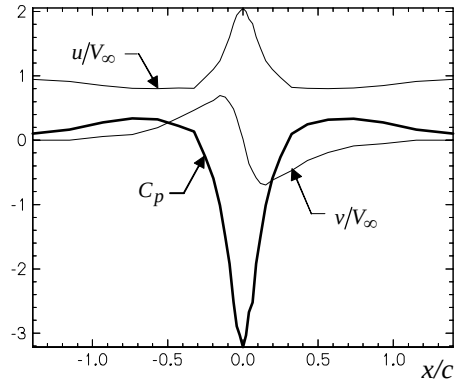

Figure 8. Flow characteristics over the surface of a smooth curve in external flow.

TABLE 1. Number of Iterations and CPU Time to Converge and the Maximum Error of Pressure Coefficient for Two Cases Shown in Figures 3 and 4.

Case	Number of Iterations	CPU time (s)	Maximum Error (%)
NACA0010-66	5	2.75	3.4
$NACA65_4$-021	6	5.94	2.1

coefficient contours and velocity vectors for an ideal internal flow in a conduit with a $NACA65_2$-015 obstacle. The pressure coefficient distribution

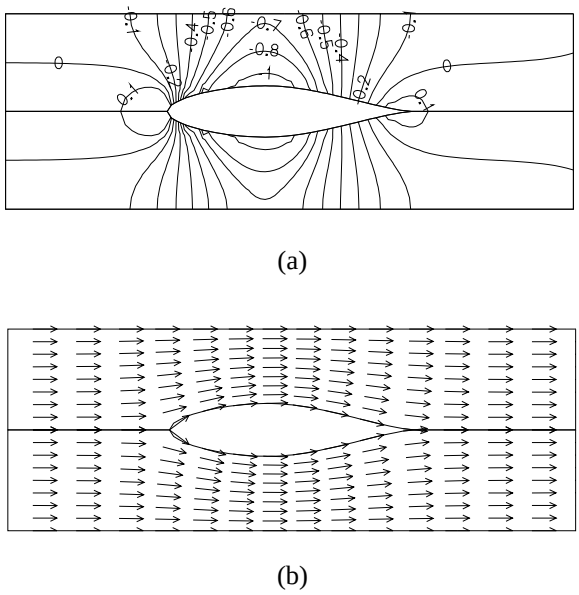

Figure 9. (a) C_p contours and (b) Velocity vectors for an ideal internal flow over NACA65$_2$-015.

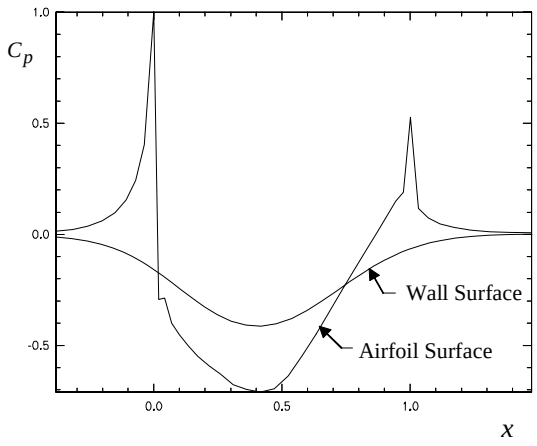

Figure 10. Pressure coefficient distribution over the wall and the airfoil surface shown in Figure 9.

over the wall and the airfoil surfaces, related to Figure 9, are shown in Figure 10.

Pressure coefficient distribution and velocity vectors for an ideal flow in a smooth diffuser are shown in Figure 11. The pressure coefficient distribution over the wall and the core surfaces of the internal flow in a diffuser, related to Figure 11, are shown in Figure 12.

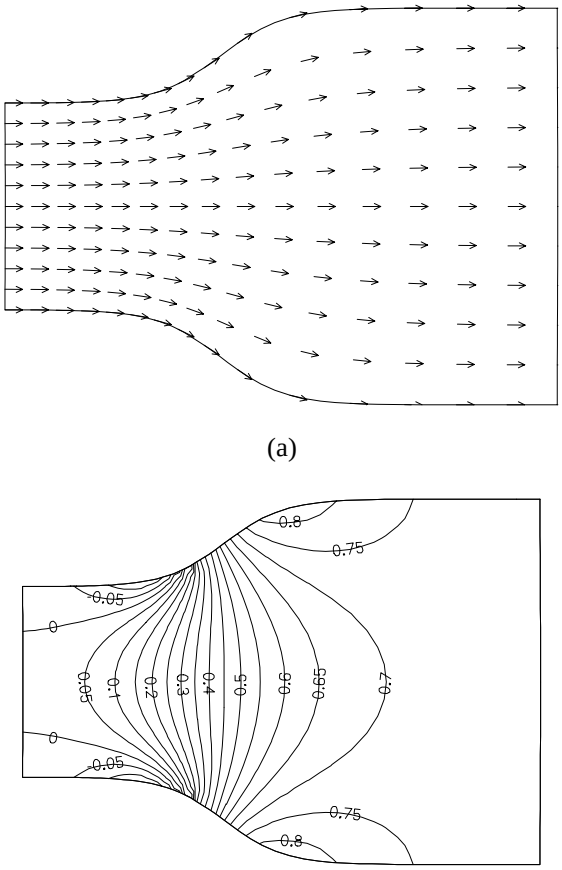

Figure 11. (a) C_p contours and (b) Velocity vectors for an ideal internal flow in a smooth diffuser (AR=0.5)**.**

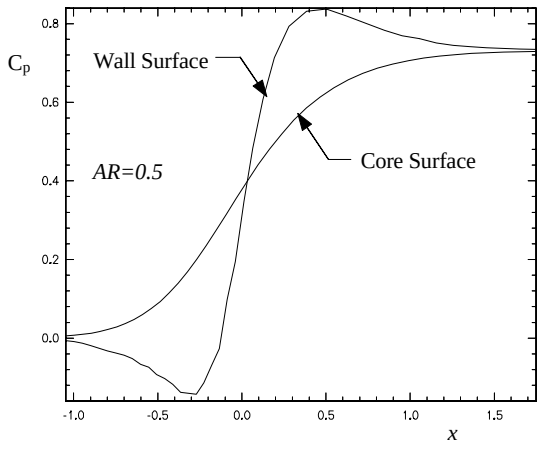

Figure 12. Pressure coefficient distribution over the wall and the core surface of the nozzle shown in Figure 11.

5. CONCLUSION

A new method based on Schwarz-Christoffel transformation for complete solution of two-dimensional ideal external and internal flows over arbitrary boundaries is developed. In this method, the components of velocity and the pressure coefficient are obtained based on the analytical functions.

The solution is independent of the coordinates of solution domain (in contrast to FDM or FEM) and is not required at some control points (in contrast to panel method).

Using this method, a solution for the body pressure and velocity distribution can be obtained without solving for the flowfield throughout the domain (like the panel method). The pressure and velocity distribution for some grid points in the solution domain can also be obtained (like FDM or FEM).

A *Mathematica* package has been developed to

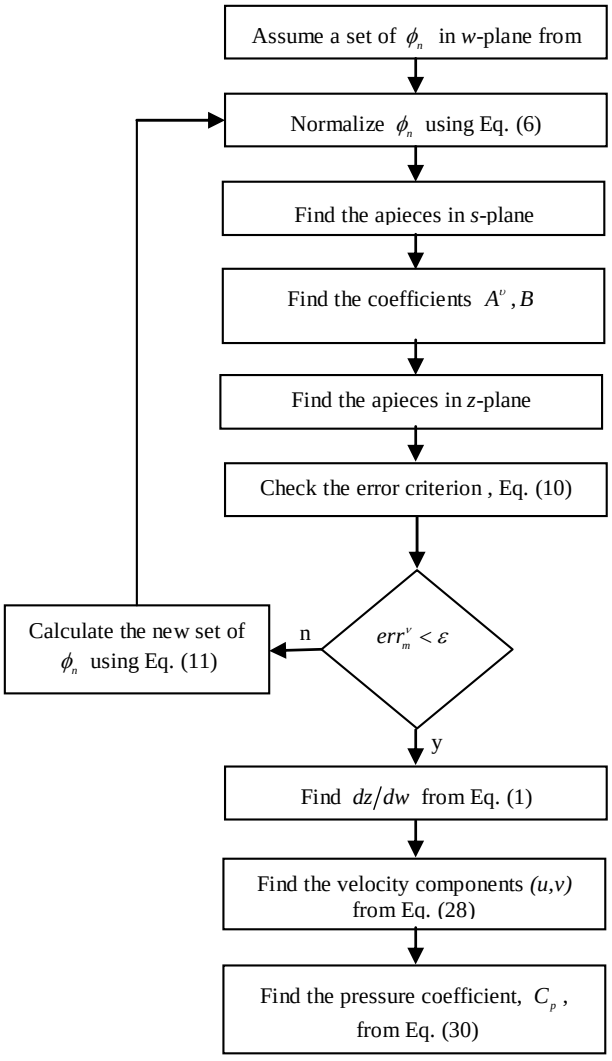

Figure 13. The flowchart of program for external ideal flows.

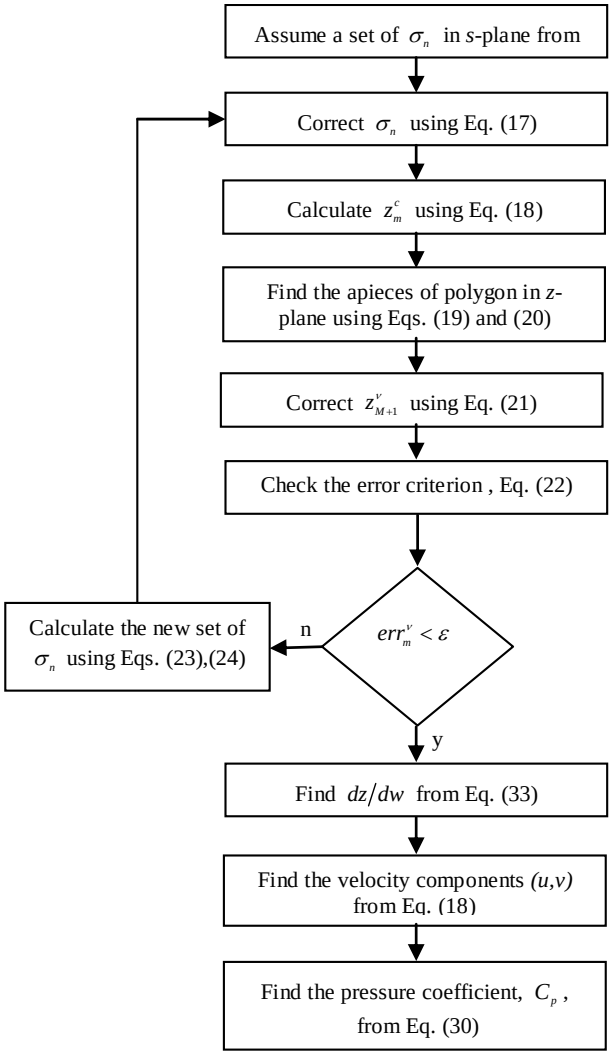

Figure 14. The flowchart of program for internal ideal flows.

perform numerical calculations for 2-D ideal external and internal flow fields with arbitrary boundaries [11]. The flowchart of the program for external and internal ideal flows is shown in Figures 13 and 14.

7. REFERENCES

1. Anderson, D. A., Tannehill, J. C. and Pletcher, R. H., "Computational Fluid Mechanics and Heat Transfer", Hemisphere Publishing Corporation, New York, (1984).
2. Fletcher, C. A. J, "Computational Techniques for Fluid Dynamics", Springer-Verlag, Berlin, (1988).
3. Katz, J. and Plotkin, A., "Low-Speed Aerodynamics", McGraw-Hill, New York, (1991).
4. Milne-Thomson, L.M. "Theoretical Hydrodynamics", 4th Ed., Macmillan, New York, (1960).
5. Thompson, J. F., Warsi, Z. U. A., and Mastin, C. W., "Boundary-Fitted Coordinate System for Numerical Solution of Partial Differential Equations, A Review", ***Journal of Computational Physics***, Vol. 47, (1982), 1-108.
6. Sridhar, K. P. and Davis, R. T., "A Schwarz-Christoffel Method for Generating Two-Dimensional Flow Grids", ***Journal of Fluid Engineering***, Vol. 107, (1985), 330-337.
7. Moayeri, M. S. and Taghdiri, M. A., "Boundary-Conforming Orthogonal Grids for Internal Flow Problems", ***Iranian Journal of Science and Technology***, Vol. 17, No. 3, (1993), 191-201.
8. Mansouri, S. H., Hosseini Sarvari, S. M., Keshavarz, A. and Rahnama, M., "An Analytical Numerical Method for Grid Generation by Mathematica", ***Proc. of 26th Annual Iranian Mathematics Conference***, Vol. 1, Shahid Bahonar University of Kerman, Kerman, Iran, (1995), 251-258.
9. Mansouri, S. H., Hosseini Sarvari, S. M., Keshavarz, A. and Rahnama, M., "Two-Dimensional Boundary-Conforming Orthogonal Grids for External and Internal Flows by Schwarz-Christoffel Transformation", ***Proc. of the Tenth International Conference in Numerical Methods in Laminar and Turbulent Flow***, Vol. 10, 21-25th July1997, Swansea, UK, (1997).
10. Abbot, Z. H. and Von Doenhoff, A. E., "Theory of Wing Sections", Dover Publisher, (1949).
11. Hosseini Sarvari S. M., "MasCad 1.2, A Mathematica Package for Grid Generation and Potential Flow Simulation", International Center for Science and High Technology and Environmental Sciences, Kerman, Iran, (1998).